DEVELOPMENTS IN NMR IMAGING

E. R. Andrew*† and J. R. Fitzsimmons†

Departments of Physics and Radiology, University of Florida
Gainesville, Florida 32611, U.S.A.

Abstract: NMR Imaging is attracting widespread attention in the medical community and its introduction into major hospitals is proceeding rapidly with about ten commercial enterprises supplying the market. Early evaluations of clinical usefulness are encouraging, especially on account of the good tissue and pathological contrast, the availability of sagittal, coronal and transverse sections, and the absence of radiation hazard. Most NMR imaging is now done by the spin-warp variation of the Fourier imaging method in both 2D (single slice and multislice) and 3D. There is much discussion concerning the optimum field strength for proton NMR imaging with fields ranging from 0.02T to 2T in actual use. Attention is being paid to contrast enhancement, use of surface coils, quantitative T_1 measurements and real time imaging. Work is being done on NMR imaging of other nuclei and an imaging of the individual spectral lines of high-resolution NMR spectra. This paper gives examples of magnetic resonance images and discusses the daily routine of a magnetic resonance facility.

This paper, delivered at the ninth ISMAR conference in Rio de Janiero, gives a general review of some recent developments in NMR imaging in the context of medicine.

Probably the most significant development in the last few years has been the widespread deployment of whole-body NMR scanners in hospitals and their general acceptance in clinical practice. At the present time there are about twenty companies developing instruments and of these about ten companies are currently supplying the market. There are now over three hundred whole-body NMR scanners installed in hospitals and clinics worldwide. There are perhaps too many companies competing in this specialized field and the market has begun to shake down; two companies, one of them a market leader, have recently gone out of business.

One consequence of these commercial developments is that physicists and chemists less frequently construct NMR whole-body instruments in their own laboratories and workshops as we used to do a decade ago. Commercial systems are better engineered and have had large sums of money spent on their development.

In the early days of NMR imaging a dozen or so different techniques were proposed but practice has now crystallized on just one or two of these. Almost all medical imaging is now done by a planar imaging technique. By this we mean that a slice or plane in the object is defined and NMR signals are gathered from the whole slice simultaneously and are processed to give an image of the slice. So first we have to define the slice to be imaged and this is usually done by the selective excitation method described by Garroway, Grannell and Mansfield (1) and by Lauterbur et al. (2). A magnetic field gradient is applied along, let us say, the Z direction, and the object is irradiated with a 90° pulse of narrow spectral width, corresponding to a narrow range of field values. So only the nuclei of the thin slice corresponding to this narrow range are excited by the 90° pulse and the remainder of the object remains untouched.

The question of how to irradiate to get a well-defined slice is actually not a trivial one and it is more often done only approximately. We have currently been engaged in Florida in calculations (Mao et al. (3)) using optimal control theory to solve the Bloch equations, which are a coupled set of three differential equations, to optimize the excitation to give slices with sharply defined edges. Some success has been achieved in this and the calculated excitation pulses are now being tested experimentally.

Having defined a slice normal to Z, we can then switch the gradient into the defined XY plane, and apply it in a series of equiangular directions in the plane and reconstruct an image from a series of 1D projections in the same way as in CT X-ray scanning. That is the 2D Projection-Reconstruction method of NMR imaging and was used by Professor Paul Lauterbur (4) in his first pioneering experiments. The method is not so much used now and has almost universally given way to the 2D Fourier Imaging method, due to Kumar, Welti and Ernst (5), which is based on Cartesian coordinates. This method is therefore more straightforward, is less prone to artifacts and is readily extended to 3D and 4D.

In the 2D Fourier Imaging method we start as before by defining a slice perpendicular to the Z direction and then apply a magnetic field gradient G_x along the X direction for a time t_x, during which the nuclear free induction decay (FID) evolves. We now switch the field gradient along Y for time t_y and read the FID to n data points during t_y (for further details see (6)). So we just apply the gradient along two orthogonal directions in the plane. Next we repeat the procedure for a different value of t_x and again collect the FID. In fact, we repeat the procedure for n different values of t_x and accumulate n x n data values. To this array of data we apply a 2D Fourier transform to get an image of n x n picture elements (pixels).

Since this procedure is central to the practical generation of NMR images nowadays, let us examine the procedure in more detail to satisfy ourselves that a 2D FT really does generate the required NMR image. Let the proton density in the slice everywhere be $\rho(x,y)$. Then, neglecting relaxation effects, the NMR signal from an element of area dx dy at (x,y) in the slice will be proportional to

$$\rho \, dx \, dy \, \exp(i\gamma Bt) \qquad (1)$$

where γ is the nuclear gyromagnetic ratio and B is the magnetic induction field at (x,y). During the time t_x

$$B = B_o + x\,G_x , \qquad (2)$$

where B_o is the value of B at (0,0). During the subsequent time t_y

$$B = B_o + y\,G_y . \qquad (3)$$

After substituting (2) and (3) in (1) and detecting the NMR signal at angular frequency $\omega_o = \gamma B_o$, the NMR signal from the element is proportional to

$$\rho \, dx \, dy \, \exp[i\gamma(x\,G_x t_x + y\,G_y t_y)]. \qquad (4)$$

For the whole slice the NMR signal is therefore

$$S(t_x,t_y) = \iint \rho(x,y)\exp[i\gamma(xG_x t_x + yG_y t_y)]dx\,dy \qquad (5)$$

$$= A \iint \rho(\omega_x,\omega_y)\exp[i(\omega_x t_x + \omega_y t_y)]d\omega_x d\omega_y , \qquad (6)$$

where

$$\omega_x = x\gamma G_x , \quad \omega_y = y\gamma G_y , \quad A = (\gamma^2 G_x G_y)^{-1} .$$

We see that the double integral in equation (6) is just the 2D Fourier transform of ρ with ω and t as conjugate variables. From the reciprocal property of Fourier transforms is therefore follows that $\rho(x,y)$, which is the quantity we want to construct the image, is just the 2D Fourier transform of $S(t_x,t_y)$, which we measure.

We should notice that in this analysis t_x always appears multiplied by G_x. So instead of incrementing t_x through n successive values, we can equally well hold t_x constant and successively increment G_x through n values, which has practical advantages. This is the spin-warp variation of Fourier imaging developed by Edelstein et al. (7). This method can readily be extended to 3D, but its 3D form has not often been used hitherto because of the long imaging time required. However, the recent advent of faster imaging methods may make 3D and selective 3D Fourier imaging more attractive. The method can also be extended to 4D, namely three spatial dimensions and one spectroscopic dimension, providing NMR spectra from any volume element and providing NMR images of any spectral line.

We now turn to some NMR images obtained on our Technicare scanner at the University of Florida hospital which uses the imaging techniques just described. This is a first generation system, in clinical use for three years, which employs a 0.15 Tesla resistive magnet (Figure 1) and operates at 6.5 MHz for proton NMR.

Figure 2 shows a sequence of proton NMR images of ten equally spaced transverse sections of the head of one of the authors (ERA). The slices are 5 mm thick. All these images were obtained simultaneously in 4 minutes by the multislice technique to be described later.

An important feature of NMR imaging is that, unlike CT X-ray scanning, the slices imaged need not be transverse to the length of the body, but can equally well be sagittal or coronal. Figure 3 shows a sequence of ten sagittal images of the head of the same author (ERA), starting with a section through the left eye, and then at equally spaced intervals moving to the midline and then on to the right eye and the right side of the head. Again these were obtained simultaneously through the multislice technique.

Figure 4 shows a set of ten sagittal images through the chest of the same author. It should be remarked that the images of the heart are blurred because of its movement. However, this blurring can be removed by synchronizing successive 90° pulses with the electrical impulses from an electrocardiograph, enabling images to be obtained of any desired phase of the heart's cycle. Figure 5 shows a set of ten transverse images through the abdomen of the same author.

These four figures show a large number of NMR images of what is believed to be a normal human body and one sees something of the spatial resolution attainable, namely 1 mm in the head and 1-2 mm in the body, using a low field, first generation instrument. There are two comments to be made at this stage.

First, we should note that the images are all proton NMR images, and in fact almost all clinical NMR imaging uses protons. Hydrogen is the most abundant chemical element in the body and the proton is almost 100% isotopically abundant with spin ½ and the highest gyromagnetic ratio of all stable nuclei. So protons give by far the best signal/ noise ratio and consequently the best image resolution. Oxygen has no suitable isotope, ^{13}C is only 1.1% abundant, nitrogen is not promising. Phosphorous ^{31}P is interesting because of its role in the body's metabolism, but it is some three orders of magnitude lower in concentration in the body than hydrogen, so you need a thousand times the volume of tissue to get the same signal/noise in the same time, which means a reduction in spatial resolution for ^{31}P imaging by ten times. So protons are far and away the favorite nucleus for imaging. Some imaging work is, however, also being done with ^{7}Li, ^{13}C, ^{19}F, ^{23}Na, ^{31}P and with electrons.

The second comment to be made is concerned with the high-resolution aspects of NMR. Most of the proton NMR

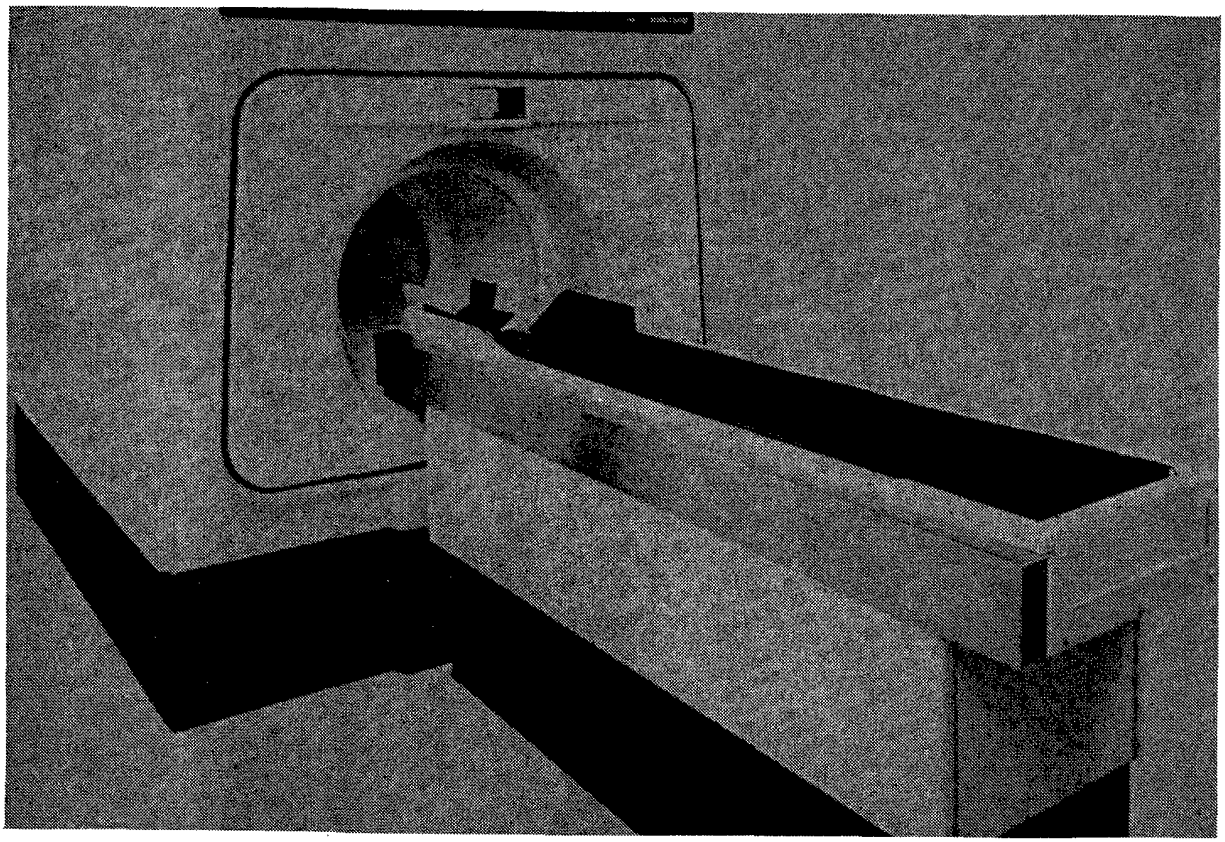

Figure 1. View of the 0.15 Tesla imaging magnet in use at the University of Florida

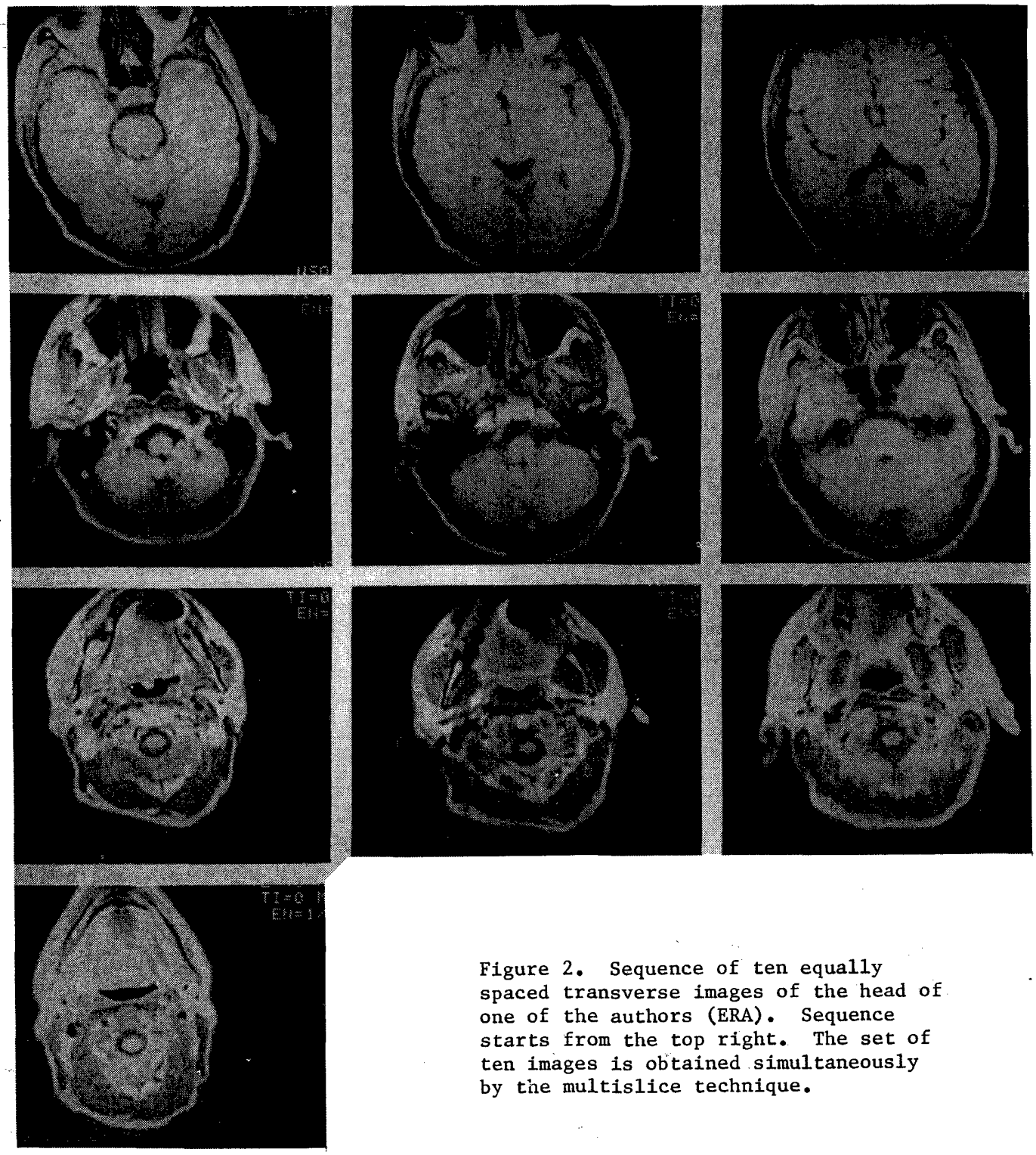

Figure 2. Sequence of ten equally spaced transverse images of the head of one of the authors (ERA). Sequence starts from the top right. The set of ten images is obtained simultaneously by the multislice technique.

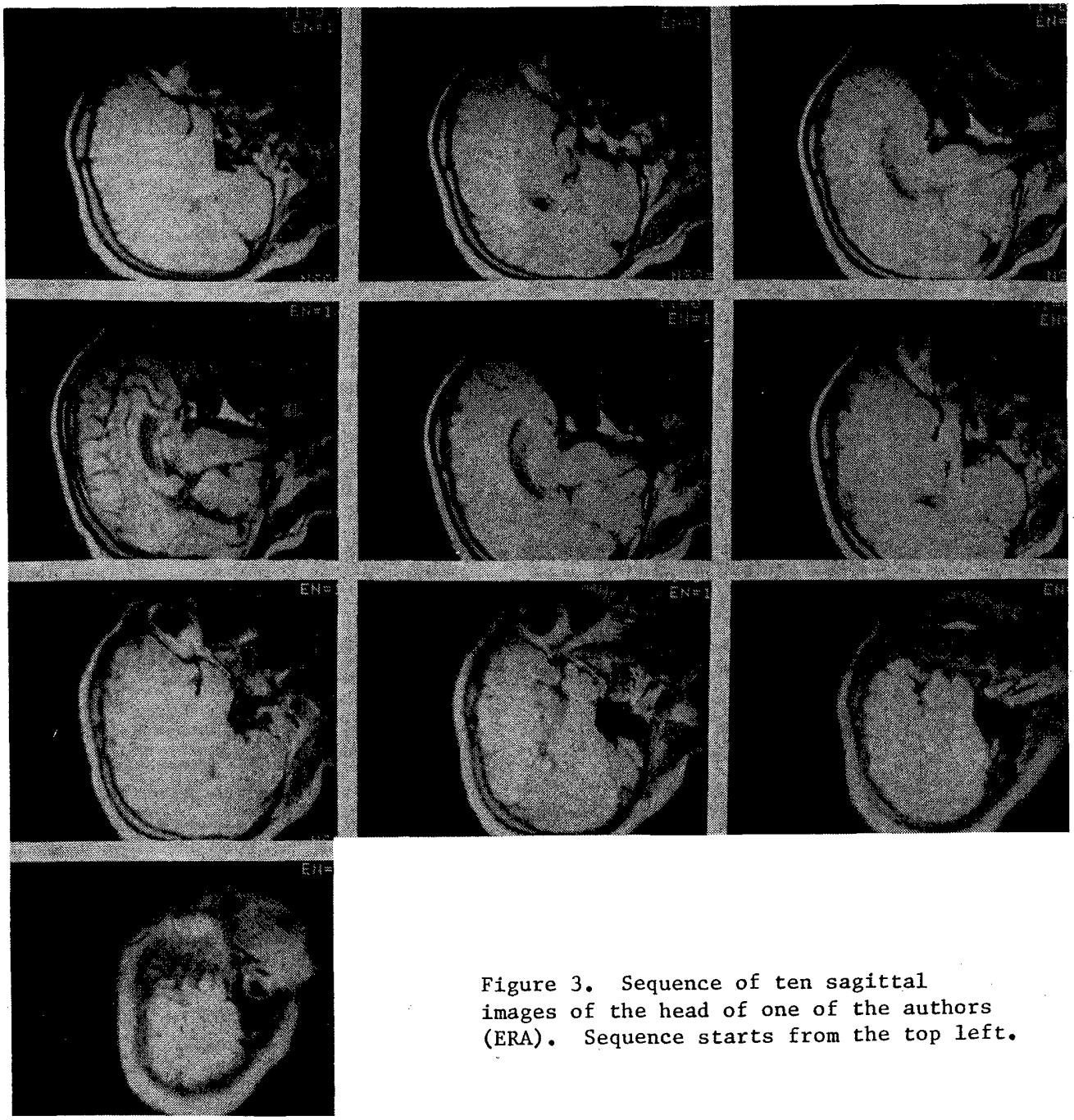

Figure 3. Sequence of ten sagittal images of the head of one of the authors (ERA). Sequence starts from the top left.

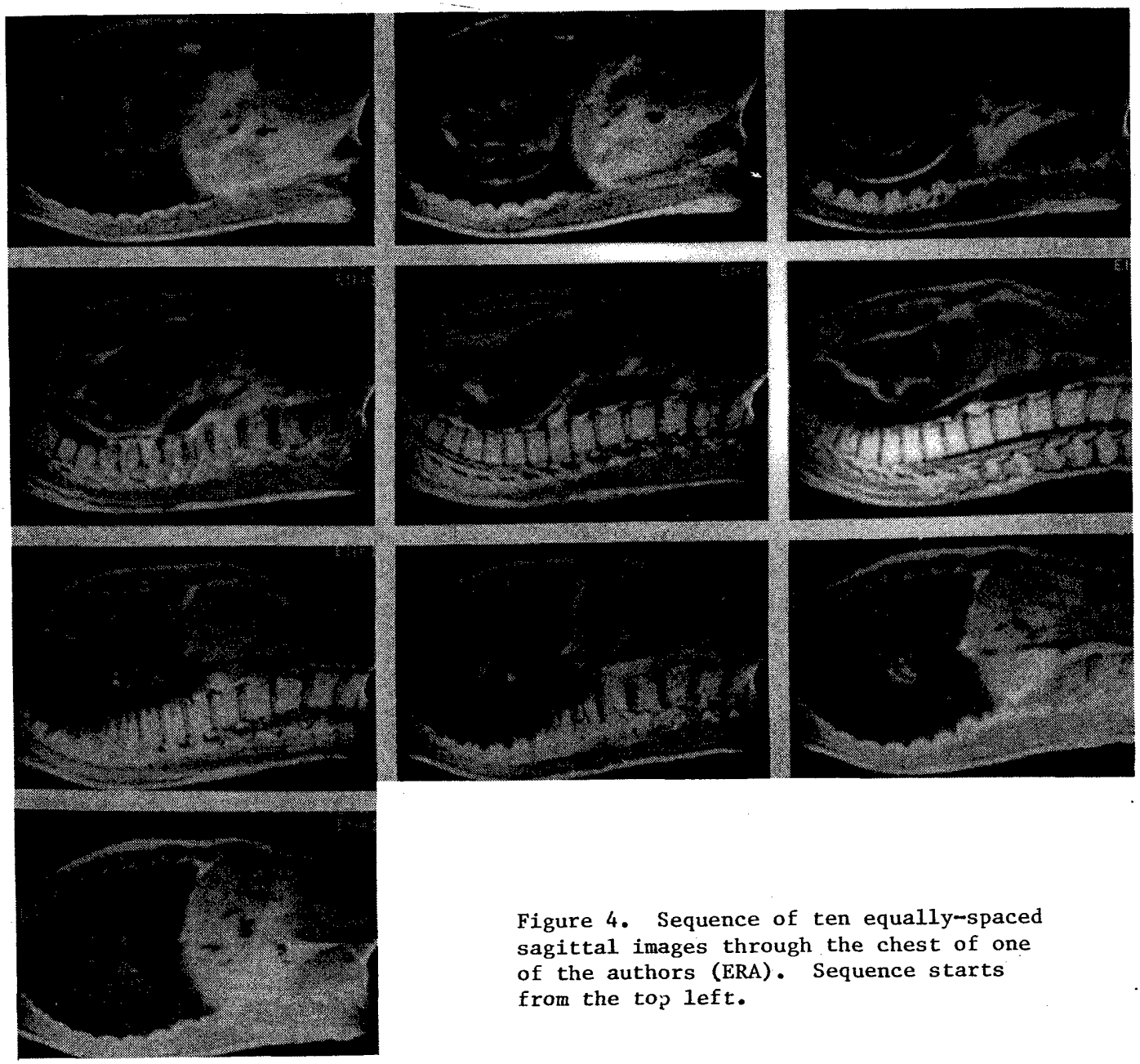

Figure 4. Sequence of ten equally-spaced sagittal images through the chest of one of the authors (ERA). Sequence starts from the top left.

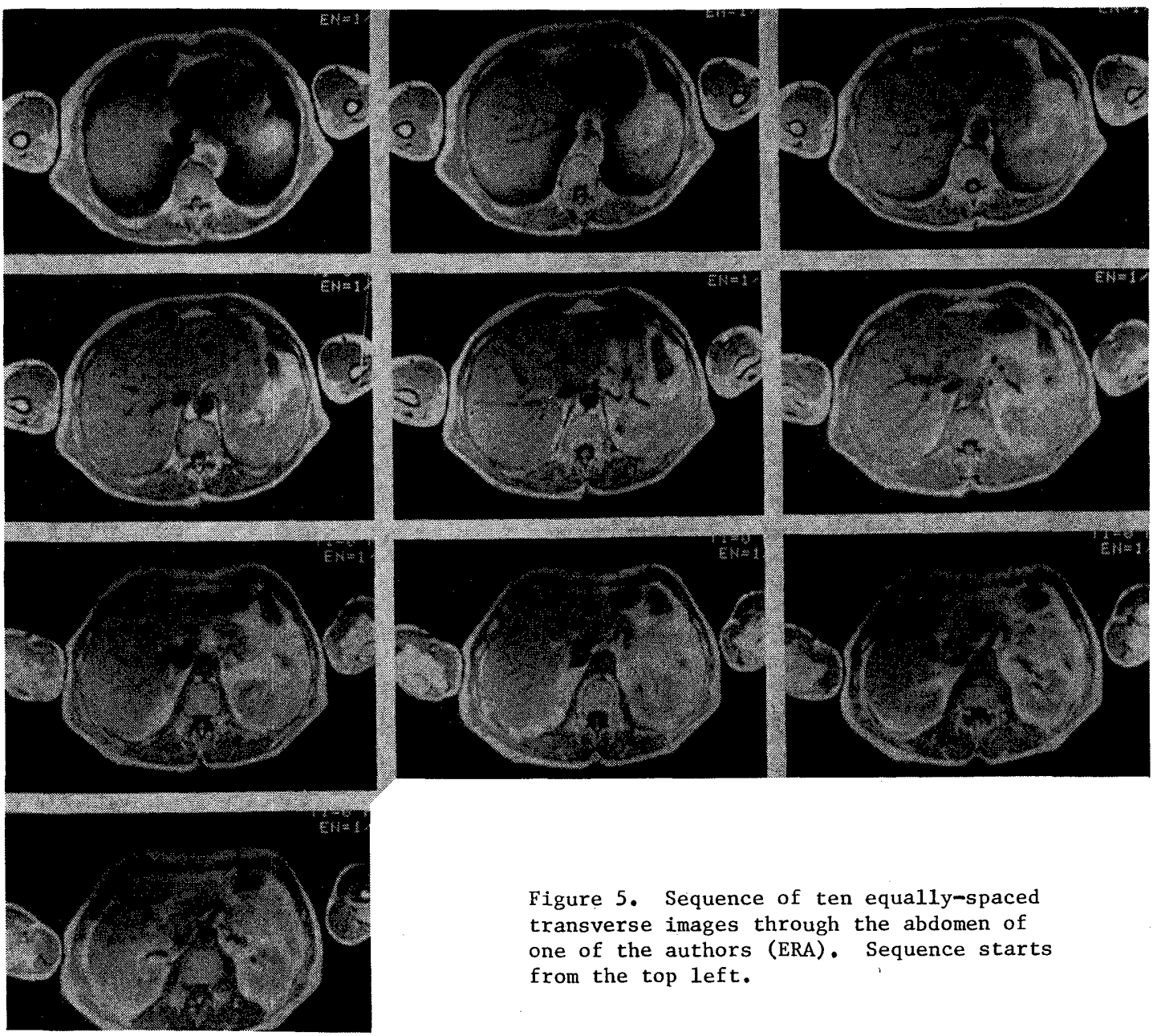

Figure 5. Sequence of ten equally-spaced transverse images through the abdomen of one of the authors (ERA). Sequence starts from the top left.

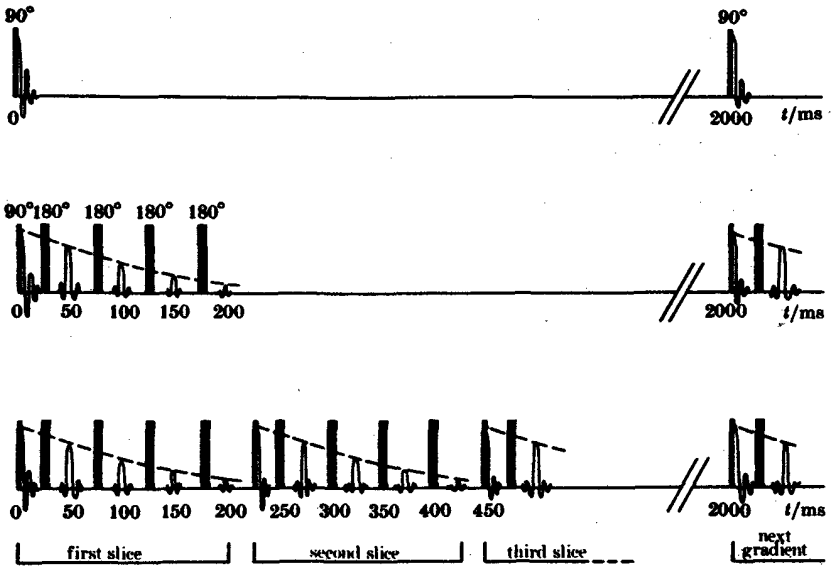

Figure 6. Diagram illustrating the multiecho-multislice procedure for the economical use of time in NMR imaging, and for obtaining T_2-weighted images.

signal comes from water and fat; all the other beautiful spectral lines which can be observed at low intensity constitute negligibly overall. Water and methylene resonances are chemically shifted about 3 ppm apart and in most imaging systems they are not resolved and we just image the total proton signal. At fields over 1T the effects of the two components can be seen and work has been done to image them separately. However, in most systems these two chemically-shifted components are regarded as a nuisance which generate artifacts which are eliminated by the use of higher field gradients.

An important aspect of NMR imaging is imaging time. CT X-ray scans are obtained in a few seconds, so this provides a challenge and a stimulus to NMR imaging to make sure that we use our time efficiently. The question of the economical use of time is illustrated in Figure 6. The top line illustrates the basic procedure for 2D Fourier imaging. A slice is selected with a 90° pulse, field gradients are applied and the FID, which may last for typically 10 ms, is read. Then we have to wait 1-2 seconds for the protons to undergo spin-lattice relaxation before repeating with new values of field gradient. In this way we can get 128 gradient values in 4 minutes if we wait 2s between pulses as illustrated in Figure 6 or 256 gradient values if we wait 1s between pulses. We see that a very large amount of time is wasted between the end of the FID and the next pulse, just waiting for spin-lattice relaxation. So is there something useful that can be done while waiting?

The first thing we can do is illustrated in the second line of Figure 6. We can insert a series of 180° pulses giving spin echoes at, for example, 50, 100, 150 and 200 ms and we can reconstruct images from each set of echoes. The echoes decay with the value of the transverse relaxation time T_2, and this will vary from one tissue to another. In particular, cancerous tissue, which often has longer relaxation times than normal tissue, as shown by

Damadian (8), will progressively stand out in later echo images. An example of such a T_2-weighted image is shown in reference (6), figure 19. However, as the second line of Figure 6 shows, even this echo sequence only uses 200 ms of the 2000 ms available, a reflection of the fact that $T_2 << T_1$ in living tissues. So what can we do with the time that still remains unoccupied?

As illustrated in the third line of Figure 6, we can now attack an adjacent virgin slice by selecting a second slice and repeating the procedure. Then we may proceed to a third slice and so on. With the parameters chosen for the figure we can examine ten slices before returning to the first slice, which will by then have fully relaxed. This is the multiecho-multislice procedure which fully uses the available time. In Florida we regularly gather four echo images of ten adjacent slices getting 40 images in 4 minutes or 6s per slice which is competitive with CT X-ray scanning. With two averages, as is customary, these times are doubled.

In this procedure it is however necessary to wait the full four minutes to get any one of these images. There are now several faster techniques under development such as the echo-planar method of Mansfield (9) and the FLASH technique of Haase et al. (10) which can generate an image in a second or less and which therefore offer the opportunity of real time movie NMR images.

The acceptance of magnetic resonance imaging (MRI) as a regular modality of radiological investigation has depended on the usefulness of the images to the clinician. One example in our hospital has been in cases of musculoskeletal tumors. In the past, treatment has usually consisted of amputation of the limb, but in recent years much more often the tumors in arms and legs are excised, but this demands very precise delineation of the tumor. Figure 7 shows an example of one of our patients with liposarcoma of the right leg. It is difficult to see the tumor in the CT X-ray scan (Figure 7a) but the longer relaxation time of the tumor enables it to be seen very clearly and precisely in the NMR image (Figure 7b). We have now seen over two hundred cases of tumors of the musculoskeletal system and the NMR images have played a major role in limb salvage surgery in these cases.

On a sequence of sixty musculoskeletal tumor patients we have measured T_1 and T_2 for the tumors (11). The relaxation parameters are obtained by fitting three or four points to an exponential recovery or decay. One would prefer to have more experimental points; with a pure material in a sample tube one might well take 20 measurements to test exponentiality and obtain a good value for the relaxation time. However, in our case we are making measurements on a live sick patient and we do not have all day. The whole clinical examination should be over in an hour and the T_1, T_2 measurements are purely incidental to the medical diagnostic work. Nevertheless, the values obtained are relaxation parameters which characterize the relaxation processes using a standard measurement procedure whose reproducibility has been tested on normal subjects of all ages under a variety of conditions. T_1, T_2 plots for different types of soft tumor (identified histologically after excision) showed that they can in many cases be distinguished with 95% confidence by their relaxation parameters. Significant changes were found in the relaxation parameters before and after therapy.

Sometimes lesions of interest do not show a significant difference of relaxation times from normal tissue and are not well discriminated. In such cases, it can be helpful to administer a contrast agent, an agent which will enhance the relaxation rate differentially and trials are being conducted on such agents in several centers including our hospital in Florida. One agent on which attention has been focussed is a solution of a gadolinium chelate such as GdDTPA (diethylene-

tetramine-penta-acetic acid). Gadolinium, being a rare earth element, has a strong electronic magnetic moment from its inner unpaired 4f electrons while the chelate grasps the outer electrons and renders the molecule unreactive and non-toxic. The strong electronic magnetic moment of these molecules enhances the relaxation rates in their vicinity. If the agent goes preferentially to the lesion it causes it to show up with improved contrast. This is particularly valuable for lesions in the brain since the agent penetrates the lesion membrane, but the large chelate group is unable to penetrate the blood-brain barrier. Our medical colleagues express a cautious optimism that such contrast agents may be useful in clinical practice in the future.

Another development in the last few years has been the use of special receiver coils which fit snugly around the part of the anatomy we are interested in and yield an improved signal/noise ratio because of their closer coupling. Examples are coils which fit closely around the neck and limbs (Fitzsimmons, Thomas and Mançuso (12)). Special coils are helpful for the female breast (6). The patient lies prone on the couch with the breast under examination falling pendant in a coil about 12 cm in diameter.

It may be of interest to describe the day's operation of our MRI scanner. At 6:30 am the technologist arrives and switches on the instrument, the magnet warms up and initial checks and adjustments are made. At 7 am the first patient arrives. It is necessary to explain the procedures to the patient, to check that he has no cardiac pacemaker and no large pieces of metal in his body. The patient is then moved into the magnet room and on to the couch, which is then inserted into the bore of the magnet until the region of interest is in the center. The technologist then takes the images requested by the referring physician. Although the magnet room has full radiofrequency screening it is usually found in practice in our very quiet environment that the door to the control room can be left wide open, allowing good contact between patient and technologist. In the case of children a parent often sits in the magnet room close to the patient. The pictures obtained are viewed by a radiologist MD on the monitor to see that they are satisfactory before the patient leaves. The whole examination takes about an hour. A second technologist comes on duty at midday and we see about ten patients a day until 6 pm, often later, about 50 a week, over 2000 a year. At 8 am the chief MRI radiologist conducts a conference at which the previous day's cases are reviewed. A report goes to the patient's physician who decides treatment. The charge for an MRI examination is $500. The scanner was purchased in 1983 for $900K, to which must be added installation costs of about $200K. Superconducting systems cost about twice as much.

Systems for MRI are available on the market which operate with magnetic fields from 0.02 Tesla to 2 Tesla, a range of a hundred-fold. The question of what is the ideal field strength to use is very much a matter of debate. Let us summarize the arguments for and against higher and lower field strengths which will have more or less appeal to different users.

There are two advantages which follow from the use of high magnetic fields. The first is improved signal/noise with consequent improvements in spatial resolution, particularly in the head. The second is improved chemical-shift resolution if the system is also to be used for in vivo magnetic resonance spectroscopy. Indeed, the highest possible magnetic field is needed for spectroscopy and certainly over 1 Tesla. For some users these will be over-riding considerations in the choice of system.

Advantages which follow from the use of lower magnetic fields are: (a) Shorter values of T_1, enabling faster pulsing which recovers some loss of signal/noise; (b) A wider range of T_1 values improving tissue contrast; (c)

Figure 7. (a) Upper picture, CT Xray scan through the thighs of a patient with a liposarcoma in the right leg (the right leg is on the left in the image). The tumor is not readily seen. (b) Lower picture, Proton NMR scan of the same patient. The tumor is clearly visible.

Absence of chemical-shift artifact. This can always be overcome by use of larger field gradients, but this requires larger bandwidths with some loss of signal/noise; (d) Lower radio frequency power deposition in the body; (e) Smaller stray magnetic fields; (f) Lower capital costs and running costs. For some users this last factor may be an over-riding consideration.

Users who do not have strong financial constraints and do not wish to engage in magnetic resonance spectroscopy often choose a superconducting system in the middle range of field strength.

This work has received support from NIH grant No. 1 P41 RR02278-01 and NIH grant No. CA 42283-01.

References.

1. A.N. Garroway, P.K. Grannell and P. Mansfield, J. Phys. C 7, 457 (1974).
2. P.C. Lauterbur, C.S. Dulcey, C.M. Lai, M.A. Feiler, W.V. House, D. Kramer, C.N. Chen and R. Dias, Proc. 18th AMPERE Congress, Nottingham 1974, Ed. P.S. Allen, E.R. Andrew and C.A. Bates, North-Holland, Amsterdam, 27 (1975).
3. J. Mao, T.H. Mareci, K.M. Scott and E.R. Andrew, J. Magn. Res. 70, 310 (1986).
4. P.C. Lauterbur, Nature 262, 190 (1973).
5. A. Kumar, D. Welti and R.R. Ernst, J. Magn. Res. 18, 69 (1975).
6. E.R. Andrew, Proc. Roy. Soc. Lond. B 225, 399 (1985).
7. W. Edelstein, J.M.S. Hutchison, G. Johnson and T. Redpath, Phys. Med. Biol. 25, 751 (1980).
8. R. Damadian, Science 171, 1151 (1971).
9. P. Mansfield, P.G. Morris, R.J. Ordidge, I.L. Pykett, V. Bangert and R.E. Coupland, Phil. Trans. Roy. Soc. Lond. B 289, 503 (1980).
10. A. Haase, J. Frahm, D. Matthaei, W. Hanicke and K.D. Merboldt, J. Magn. Res. 67, 258 (1986).
11. E.R. Andrew and H.T.A. Pettersson, Magnetic Resonance in Cancer, Ed. P.S. Allen, D.P.J. Boisvert and B.C. Lentle, Pergamon Press, Toronto 37 (1986).
12. J.R. Fitzsimmons, R.G. Thomas and A.A. Mancuso, Magn. Res. Med. 2, 180 (1985).